

Accumulation of Explosive in Hair: Part 3: Binding Site Study ^{1,2}

Oxley^{*a}, J.C.; Smith^a, J.L.; Kirschenbaum^a, L.; Marimiganti^a, S.; Efremenko^b, I.; Zach^c, R.; Zeiri,^{c,d,*Y}

^a Department of Chemistry, University of Rhode Island, Kingston, RI 02881

^b Department of Organic Chemistry, Weizmann Institute of Science, 76100 Rehovot, Israel

^c Department of Biomedical Engineering, Ben Gurion University, Beer Sheva 84105, Israel

^d Department of Chemistry, NRCN, P.O. Box 9001 Beer Sheva 84190, Israel

* Corresponding authors

Abstract

Previous studies have shown that hair can serve as a good template for binding a variety of explosives.

This study addresses the possible mechanisms responsible for the binding of different explosives to the hair surface. Based on previous studies suggesting 2,4,6-trinitrotoluene (TNT) and triacetone triperoxide (TATP) may adsorb to hair differently, this study used only these two explosives as exemplars. The experimental approach was to chemically treat hair in different ways and determine how this affected explosive sorption and morphological changes of the hair surface. Treatments examined include moistening; rinsing with acetonitrile or methanol; bleaching with hydrogen peroxide and alkaline hydrogen peroxide; and treating with a methanolic KOH solution or potassium permanganate. The morphological changes of the hair surface following these treatments were examined using both scanning electron microscopy (SEM) and tapping mode atomic force microscopy (TM-AFM). The results of these studies suggest that the adsorption of both TATP and TNT are markedly affected by the treatment of hair with the different chemicals used in the rinsing process. The examination of the hair surface using TA-AFM clearly shows different degree of smoothing following the rising treatment. This supports the suggestion that the explosive molecules attachment to hair is largely a surface phenomenon involving the 18-MEA lipid layer. The large differences in the amounts of TNT and TATP adsorption are associated with the marked differences in vapor pressure of these two explosives. In the case of TATP adsorption it was found that micro-crystals of the explosive were formed on the hair surface. Density functional theory (DFT) calculations were employed to explore possible nucleation sites of TATP micro-crystals on the hair. It is found that some of the sites

on melanin granular surfaces may support nucleation of TATP micro-crystals. The theoretical results, in conjunction with recent findings on ethnic differences in hair surface structure and composition, support the experimental finding that dark hair adsorbs explosives better than light hair.

Introduction

In previous studies of the sorption of explosive vapors by hair^{1,2}, we made a number of observations which lead to speculation concerning the mechanisms responsible for the sorption of explosives to hair. Based on these previous studies we noted some general features associated with sorption of explosive onto hair surfaces:

1. a general color bias--black and red hair sorbed explosives more readily than brown or blond hair;
2. poor sorption of explosives by bleached hair;
3. poor sorption of explosive by white hair compared to black hair from the same person;
4. an individual preference for explosives, i.e. if a person's hair sorbed one explosive readily, it sorbed all explosives readily;
5. substantial differences in amount of explosive sorbed by hair compared to cotton balls, wool, polyester, silk, and Nylon;
6. the observation that high vapor pressure explosives, such as TATP, appear to be readily rinsed from the surface of hair, but low vapor pressure explosives, such as TNT, appear to require more vigorous agitation;
7. the observation that melanin sorbs both TATP and TNT more readily than some of the best performing black hair;
8. initial sorption of explosive occurs at a rate proportional to the vapor pressure of the explosive;
9. initial sorption of any of the explosives is rapid; but explosive uptake continues at a much slower rate for long periods of time, i.e. many months.

Since hair appears to be more than a template on which a subliming explosive can condense, the structure of hair must be considered. Hair structure includes a medulla, an inner cortex, and an outer

shell, called the cuticle. Melanin granules, responsible for the hair color, are found almost exclusively in the inner cortex layer. There are two types—eumelanins, the brown-black pigments; and pheomelanins, the yellow-red pigments. The cuticle of hair and, indeed, the outermost layer of skin and nails consist of a fibrous protein known as keratin. However, the outer surface of mammalian hair has a more complex structure than skin or nails. The cuticle is a hard, transparent shingle-like layer made up of 9 to 10 sheet-like cells, called scales, which are 0.5 μm thick and stacked over each other. Each scale has a laminar structure with an outer and an inner layer, named respectively the exo- and endocuticle.³ The epicuticle consists of proteins rich in cysteine, which can crosslink via disulfide bonds to form cystine.⁴ In hair, this bond occurs about every four turns of the α -helix. Depending on the ethnic origin and the individual, the layers of the cuticle can range from approximately 7 to 16, resulting in hair diameters from 18 to 180 μm . The surface of the scales is covered by a thin layer (~ 3 nm thick) of lipids, the β -layer.⁴ This layer constitutes a monolayer of saturated fatty acids, the most abundant being 18-methyleicosanoic acid (18-MEA).^{5,6} 18-MEA is thought to be covalently bound, possibly via a thioester linkage, to the cystine-containing proteinaceous outer surfaces of mammalian keratin fibers.^{7,8} The purpose of this unusual branched-chain fatty acid monolayer is unknown, though it is speculated that by disrupting the monolayer packing, it imparts beneficial tribological properties.

The interaction of explosives with a multi-functional, biological structure, such as hair, is quite complex. Observations 1, 2, 3, 6, and 7, cited above, suggested that melanin may be involved in adsorption of explosives to the hair. However, melanin is found mainly in granules relatively deep in the inner cortex. This paper presents experimental data and computational analyses aimed at pinpointing the location of explosive interaction with the hair. In previous work the computational analysis focused on the reversible and relatively weak adsorption, namely physisorption of explosive molecules onto the hair surface governed by van der Waals and Coulomb interactions. Such adsorption mechanism does not involve chemical transformations of the adsorbate or the surface. The computations indicated that the thermodynamically stable site for explosive sorption is not the hair

protein but the lipid layer, which is modeled as 18-MEA.⁹ Many of the treatments which affect hair color coincidentally are related to lower the 18-MEA content on the hair surface. Estimations of explosive adsorption capacity of the hair surface showed⁹ that the experimentally observed TATP adsorption onto some types of hair exceeds the monolayer coverage by orders of magnitude. Moreover, it was found experimentally that, in contrast to traditional nitro-group containing explosives (TNT, PETN, RDX, EGDN, NG), peroxide-based explosives (TATP and DADP) can form microcrystalline grains on surfaces of black oriental hair. To explore possible mechanisms that could lead to such behavior of the peroxide based explosives, DFT calculations were performed to examine the interaction of TATP molecules with different possible active centers on the hair surface and the possible influence of these sites on nucleation of TATP microcrystallines.

Experimental Section

Head hair was obtained by donation or purchased from Demeo Brothers, NY. In the URI lab the hair was rinsed repeatedly with sodium dodecylsulfate (SDS), distilled water, dried, and stored in Ziploc[®] bags. At BGU the SDS wash was deleted. 2, 4, 6-Trinitrotoluene (TNT) was obtained from military sources; triacetone triperoxide was synthesized in the lab. All solvents are reagent grade.

Exposure of Hair to Explosives: Hair samples were placed in sealed glass containers such that there was no direct contact with the explosive.² Samples were allowed to stand at room temperature for 48 hours. After exposure, the hair was extracted with acetonitrile, and the extracts were analyzed for explosive concentration, as described below. Usually, hair was used only once and then discarded; however, for the sequential exposure tests, after acetonitrile extraction, the hair was dried on a paper towel overnight at room temperature and then re-exposed to the explosive vapors for 48h.

Special Treatment of Hair: After hair had been cleaned, as described above, it was placed in the desired solvent system and agitated 1 to 12 hours on a shaker (86 shakes/min.). Hair was removed from the solvent with forceps and dried on paper towels overnight at room temperature. The solvent systems used included acetonitrile, methanol, methanol-KOH; KMnO₄ and hydrogen peroxide, with or

without sodium hydroxide. To remove 18-methyleicosanoic acid (MEA) black hair was immersed in a 0.1 M solution of methanol- KOH (15 mL) and shaken (86 shakes/min) at room temperature for 1 hour. Black hair was bleached by soaking overnight in 8% H₂O₂ (hydrogen peroxide), both with and without 0.1 M NaOH (an alkaline solution).

Quantification of explosives sorption: After exposure to the explosive vapor the hair samples were divided into three portions (~0.05 g each) and weighed into amber, 16 mL, screw-cap bottles. Acetonitrile (5 mL) was added, and the samples were sonicated for 20 minutes before being placed on a shaker (speed 86 shakes/minute). After shaking overnight, the acetonitrile was removed from the hair using a Pasteur pipette, and 1 mL of solution was put in a 2 mL, septum screw-cap vial. All acetonitrile extracts were analyzed on a Hewlett Packard (HP) 5890 gas chromatograph (GC) or an Agilent 6890N GC using an electron capture detector (ECD) or micro-ECD, respectively. The column used was a J&W Scientific DB-5MS column [8 m x 0.53mm (megabore), film 1.5 μ m] (HP) or a HP-5 (20 m x 0.25mm, capillary column, Agilent) or DB-5MS (25m x 0.25mm, capillary column, Agilent). The injector and detector temperatures were 165 and 300°C, respectively. Initial and final oven temperatures were 120 and 220°C, respectively; and hold times were 2 min followed by temperature ramps of 20 deg/min. An external standard method was used to quantify samples. Standard curves were constructed (using 5 points between 0.01 and 1.0 ppm) based on peak height and peak area. The squared correlation coefficients for the standard curves were better than 0.99. Both height and area data gave comparable results.

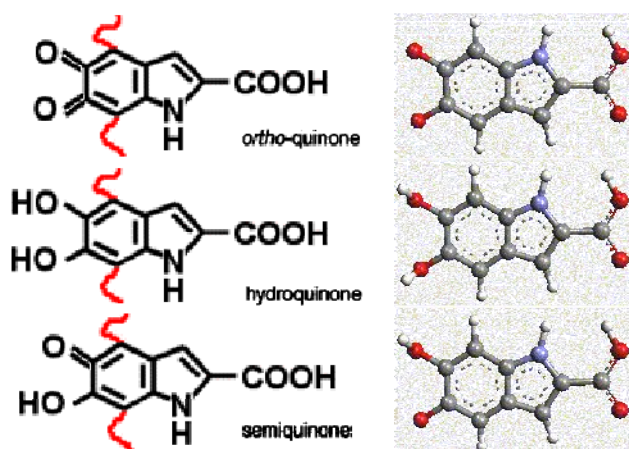
Scanning Electron Microscope (SEM): A JOEL 5900 scanning electron microscope was used to study the morphology of untreated and treated black hair. Hair strands were coated with gold before being observed under the microscope. Images were observed at 1000X magnification at an accelerated voltage of 15 keV. (Attempts to use 5000X magnification destroyed the samples.)

Atomic Force Microscope (AFM) measurements: Tapping mode AFM measurements (TM-AFM) were performed at ambient conditions using a Digital Instrument Dimension 3100 mounted on an

active anti-vibration table. A 100 μm scanner was used. Micro-fabricated silicon oxide NSC11\50 type tips (ultra-sharp) were used. The images were taken in tapping mode with a scan size of up to 20 μm at a scan rate of 0.5-1.0 Hz. The measurements reported below include height, amplitude and phase images allowing us to obtain information about the topology of the scanned areas as well as about the changes in the chemical composition of the scanned area. AFM measurements of hair surface have been reported.^{10,11,12,13,14} However, to the best of our knowledge; this is the first time that tapping mode AFM measurements are used to investigate the influence of various solvent treatment on the hair surface morphology and composition.

Theoretical method

DFT calculations were performed using the locally modified version of the GAUSSIAN03 package¹⁵. Detailed description of the computational methods was presented elsewhere.⁹ Cys and Glu centers on the protein at the hair surface were modeled by single amino-acid molecules. The exact structure of melanins has not been fully elucidated¹⁶. However a new representation of melanin structural model, based upon aggregation of oligomeric units, has been proposed recently that adequately describe the optical absorption spectrum of eumelanins. Melanins, especially eumelanins, exhibit marked redox properties, and electron delocalization between ortho-quinone and catecholic moieties of the polymer give rise to semiquinone free radicals, which can be detected by electron spin resonance spectroscopy^{17, 18}. Three monomers, ortho-quinone (OQ), semiquinone (SQ), and hydroquinone (HQ), shown in Scheme 1, were used to model the melanin centers. Similar models were applied in the DFT study of structure and adsorption spectra of eumelanin¹⁹.



Scheme 1 Structure of indolic melanin (left) & model compounds used to represent key units (right).

Results and Discussion

Effect of solvent treatment of hair on explosive sorption

Water Treatment: The hair used in these studies was washed and dried prior to use. However, we thought that some of the differences in explosive sorption exhibited by hair of the same color might be due to differences in moisture content. Therefore, some portions of hair were allowed to stand over water for 48 hours. The effects of increased moisture content on TATP and TNT sorption to hair is shown in Figures 1 and 2. Hair, which sorbed substantial amounts of TATP (1307 and 699 ug / g hair), did not experience an increase in sorption when moistened (1194 and 691 ug/ g hair, respectively), but hair which sorbed TATP poorly, such as the purchased hair, showed increased sorption when moistened. The sorption of purchased hair exposed to TNT was not improved by moisture; in fact its sorption was worsened.

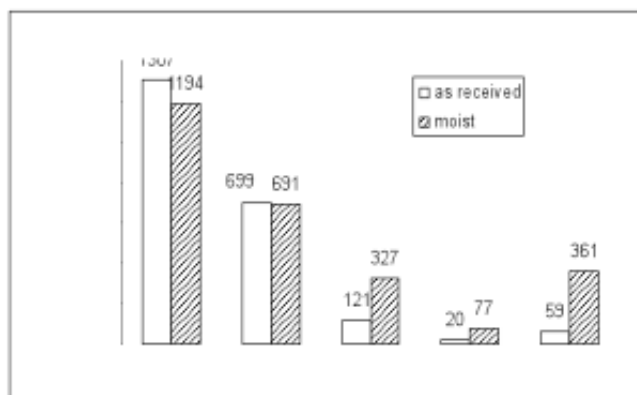


Fig. 1. Effect of moisture on TATP sorption

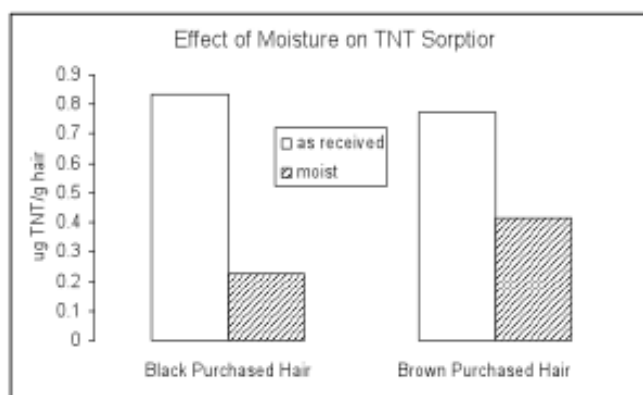


Fig. 2. Effect of moisture on TNT sorption

Acetonitrile or Methanol Treatment of Hair

The usual protocol for hair specimens, after exposure to explosive vapor and extraction with acetonitrile, was to discard the hair. Because we hoped to re-use some of the rarer hair samples, the following experiments were attempted. Instead of discarding the hair after acetonitrile extraction, it was allowed to dry and be re-exposed to the explosive vapor. The re-used hair showed an extremely reduced tendency to sorb TATP (Fig. 3). As a result, the effect on TATP and TNT sorption of rinsing hair with acetonitrile or methanol was examined. The treatment with either organic solvent greatly reduced the sorption of TATP by hair which had previously been quite sorptive. Surprisingly, the hair, which initially did not sorb TATP very well (less than 100 μg TATP/g hair), was not much affected by the organic rinses. Furthermore, the use of organic solvents reduced the degree to which TNT was sorbed only slightly (Table 1).

Effect of Hair Color Loss: Graying Hair: We had previously noted that, in general, black hair sorbed all explosives better than brown or blond hair.^{1,2} Individual variations in hair's sorption ability were observed across all explosives tested, i.e. if one sample of hair sorbed an explosive poorly, it sorbed all explosives poorly. Therefore, an effort was made to acquire hair, in this case beard hair, from a person having both white and black hairs. Table 2 clearly shows that the black hair preferentially sorbed the explosives. When black hair was artificially lightened by use of bleach, the bleached hair sorbed substantially less explosive than the unbleached hair (Table 2).

Table 2: Sorption by Black vs. White or Whitened Hair

Exposed to Type Hair	TATP 48 h		TNT 940 h	
	TATP (ug/g hair)	std dev	TNT (ug/g hair)	std dev
unbleached black	1258	70	214	20
H ₂ O ₂ bleached black	394	66	50	8
NaOH, H ₂ O ₂ bleached black	625	31	73	12
black hair	645		312	18
white hair	467	26	158	21

While treatment of hair with organic solvents or water had very different effects on sorption of TATP (decreases it) and TNT (no effect), treatments which affected hair color reduced sorption of both TATP and TNT. Hair color is attributed to melanin, a minor component of hair (~2%) found in the cortex. Bleaching agents lighten hair by attacking melanin. However, the oxidation caused by the bleaching agents is not strictly selective for the chromophores in the hair pigment. The bleaching agents can also oxidize the disulfide bonds of the surface proteins. Wolfram demonstrated that although hydrogen peroxide reacts faster with the hair pigment than the hair protein, it first reacts with the protein since bleaching agent must pass through the cuticle before it encounters the pigment.^{20,21} Experiments quantifying the rate of reaction of peroxide with pigmented versus non-pigmented hair

showed that initially (~10 min) the rate of reaction was similar because the initial reaction was with the proteins at the surface of the hair, where no pigment was found. At longer times, pigmented hair degraded peroxide faster. This is presumably due to the requirement that the peroxide needs time to diffuse to the interior of the hair to interact with the hair pigment.^{20,21}

There are a number of potential bleaching agents. In terms of the decolorizing power of the oxidizing agent on melanin, Wolfram²⁰ ordered the oxidizing agents as permanganate the greatest, hydrogen peroxide the weakest, and hypochlorite and peracid, as intermediate. However, he noted that penetration of the melanin-containing granules was an important consideration and alkaline hydrogen peroxide was effective in dissolving the granules. There are also a large number of potentially oxidizable sites on the hair protein in the cuticle and cortex. Bleaching with alkaline (NaOH) hydrogen peroxide (H₂O₂) or with alkaline peroxide/persulfate has been shown to alter amino acid composition by lowering the cystine and raising the cysteic acid content via oxidation of the disulfide linkages.^{21,22,23} While it is well-known that bleaching oxidizes the cystine residues, there is some controversy whether bleaching also removes 18-MEA. Attempts to remove 18-MEA by completely soaking hair in a methanolic solution of KOH also partially oxidize the cystine groups to cysteic acid.²⁴

The above discussion suggests that while bleaching may alter explosive sorption by degrading the melanin; it is also likely to affect explosive sorption by altering the hair surface. The reason white hair sorbs explosive poorly compared to black is likewise ambiguous. The poor sorption ability of white hair could reflect the lack of melanin, but it has also been reported that gray hair has reduced levels of 18-MEA. Furthermore, the slight ethnic bias in explosive sorption might also be attributed to racial differences in 18-MEA content, African hair having the least. Given these considerations, different hair bleaching methods were used. All methods reduced the ability of hair to sorb both TNT and TATP (Table 3).

Table 3: Black Hair (Asian Female): Effect of Different Treatments on Explosive Sorption

Explosive	Untreated		CH ₃ CN only		MeOH only		0.1MKOH/MeOH		H ₂ O ₂		H ₂ O ₂ / NaOH		KMnO ₄	
	ug Explosive/ g hair	Std Dev	ug Explosive/ g hair	Std Dev	ug Explosive/ g hair	Std Dev	ug Explosive/ g hair	Std Dev	ug Explosive/ g hair	Std Dev	ug Explosive/ g hair	Std Dev	ug Explosive/ g hair	Std Dev
TATP	684	28	246	41	---	---	nd	nd	---	---	---	---	---	---
TATP	1258	70	---	---	---	---	---	---	394	66	625	31	---	---
TNT	20	5.7	19	0.3	7	1.8	4	0.2	---	---	---	---	---	---
TNT	31	1.2	---	---	---	---	6	0.7	---	---	---	---	---	---
TNT	36	6.7	40	4.2	---	---	nd	nd	---	---	20	3.5	16	2.4
TNT*	214	20	---	---	---	---	---	---	50	12.0	73	7.9	---	---

TATP exposure was 48 h; TNT was 144 h. TNT* was exposed 940 h.

Me/KOH is KOH in 0.1M methanol; H₂O₂ is 3% peroxide except where * is 8% peroxide;

KMnO₄ is a 0.03M aqueous solution; nd=none detected

Results in Table 3 indicate that TATP sorption was adversely affected by all hair treatments. With the exception of acetonitrile, sorption of TNT was also reduced by the treatment methods. It appears that rinsing of the hair with organic solvent may not have affected TNT sorption at all, but bleaching did reduce its sorption. To accentuate the TNT results Figure 4 compares the sorption of untreated to treated hair where TNT vapors are enhanced by holding the exposure chamber at 70°C. These results clearly show that the adsorption of TNT is much greater on water-treated hair as compared to methanol-KOH treated hair. These results also suggest the reason purchased hair exhibited poor sorption of both TATP and TNT (Table 1, last four rows), since commercial hair is processed to add gloss and to remove and resist bacterial and insect contamination (e.g. with naphthalene).

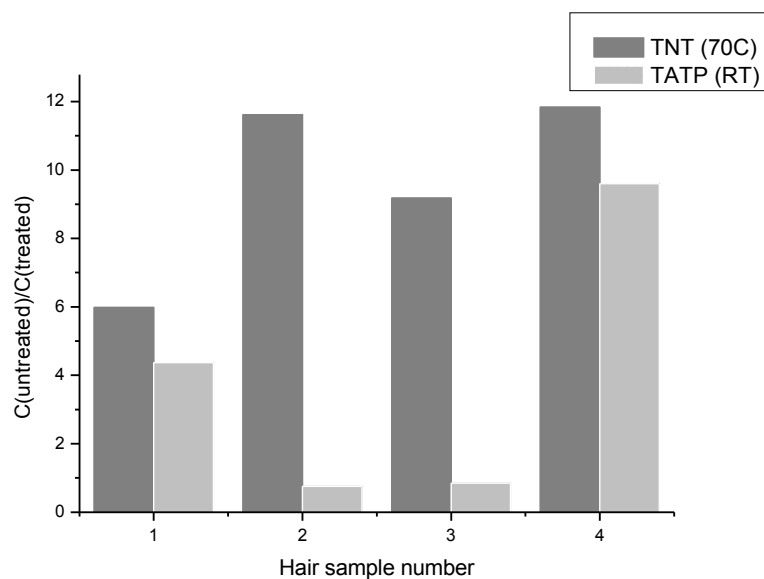


Figure 4: Ratio of explosive sorption untreated to treated (methanol-KOH) hair

Visualization of Hair Surface

SEM: In an attempt to understand how various treatments affected the sorption of explosive by hair, SEM images (1000X) were taken of untreated Asian black hair and the hair treated with various solvents (Figs. 5-8). Unfortunately, little difference could be seen between the surfaces of the untreated and the treated black hair. Therefore, TM-AFM was performed.

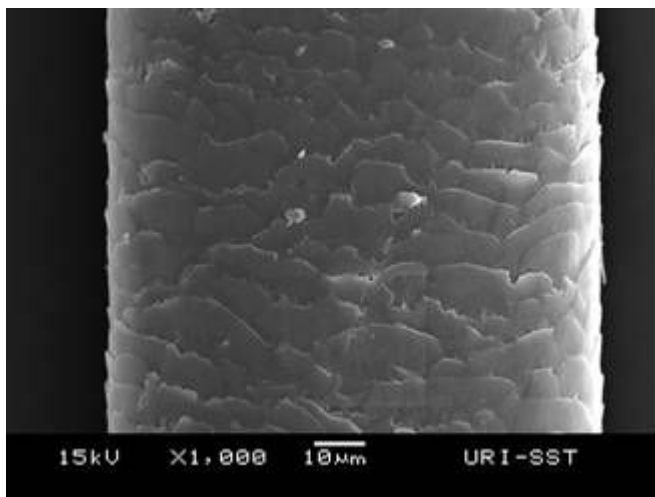


Fig. 5: Untreated Asian black hairs

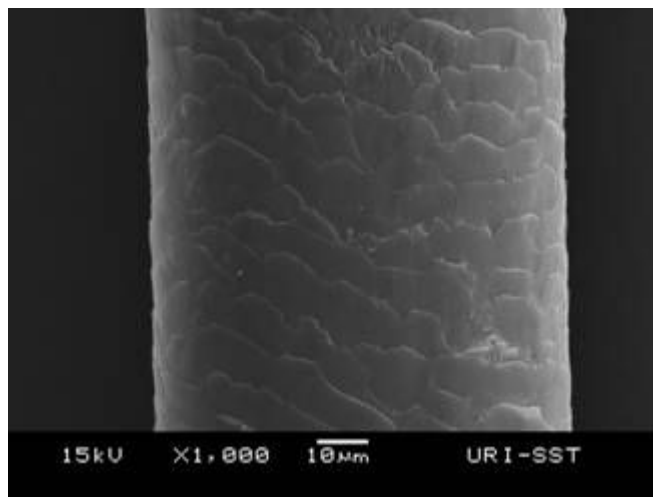


Fig. 6: Asian black hair treated with acetonitrile

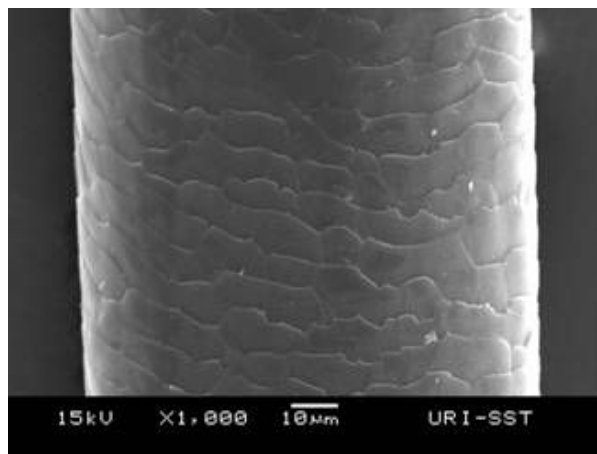
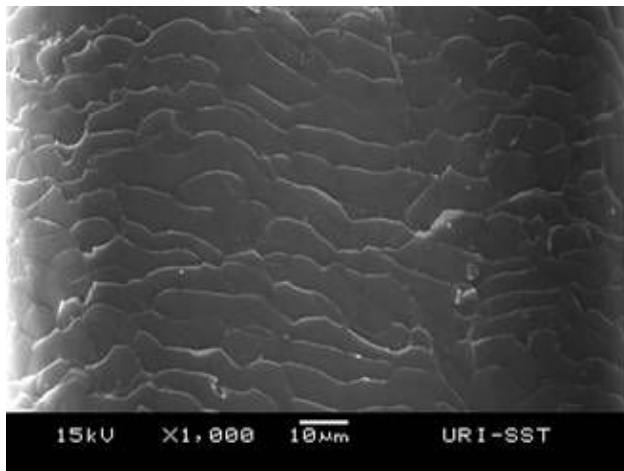


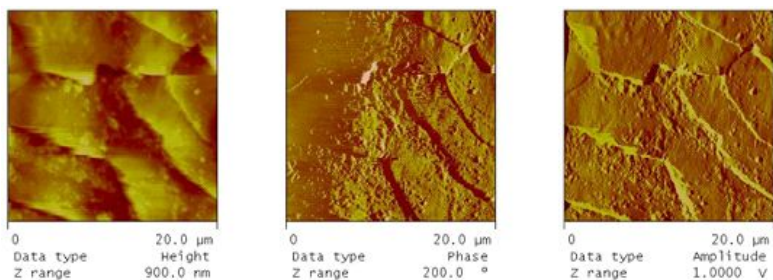
Fig 7 Asian black hair treated with 8% H₂O₂ in 0.1M NaOH Fig 8 Asian black hair treated with 0.1M methanoic KOH

TM-AFM measurements: Hair soaked in four different solvent systems, including water was examined by TM-AFM. Large area scans of dimensions 20 x 20 µm and 10 x 10 µm were performed. In most cases, these large-area scans covered an area containing more than a single scale. A set of typical results are shown in Figure 9. Inspection of these images clearly shows that the hair sample rinsed only in distilled water has the roughest surface (top left scan), while the sample treated by methanol-KOH solution is extremely smooth. The samples treated with the other two solvents are rougher than the one rinsed in methanol-KOH, but they are smoother than the one treated by water only. The images in the middle column show the root mean square changes in the cantilever amplitude during the scan. These images tend to enhance edges of on the surface examined. This can be clearly observed by the enlarged roughness on the scale surfaces as well as in the transition from one scale to another. The phase images monitor the changes in phase offset of the input drive signal with respect to the phase offset of the oscillating cantilever. The phase offset between the two signals is defined as zero for the cantilever oscillating freely in air. As the tip engages the sample surface, the phase offset of the oscillating cantilever changes by some angle with respect to the phase offset of the input drive signal. When regions with different elasticities are encountered on the sample surface, the phase angle between the two signals is changed. These changes are due to different amounts of dumping

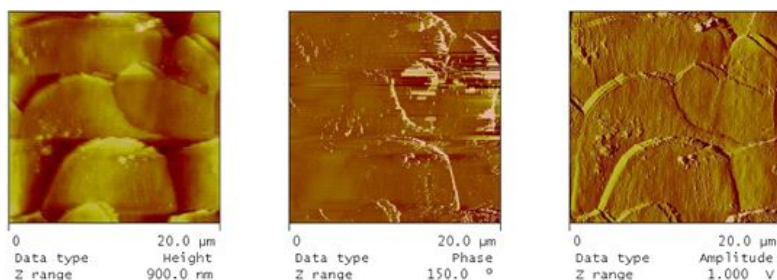
experienced by the probe tip as it rasters across the sample surface. Again, the largest variation in the phase images is obtained for distilled water rinsed samples, and the smallest variation for the sample treated by methanol-KOH solution. Note that at the scale edges the largest phase changes are observed for all four samples. This might be due to enhanced adsorption of water (or other solvent) along the scale edge.

A set of enlarged scans of these samples are presented in Figure 10. The scans span $2 \times 2 \text{ }\mu\text{m}$ and were performed on the surface of a single scale away from the scale edge. As observed in Figure 10, the sample that was only treated with distilled water showed the largest surface roughness, while the one treated with methanol-KOH solution was by far the smoothest. These features are seen clearly in both height and amplitude images (left and middle columns). The phase change images show that, except in the case of the methanol-KOH treatment, where the hair surface was highly uniform, the samples exhibited small domains where elasticity is different from most of the surface. These results may indicate the complete removal of the 18-MEA layer in the case of the methanol-KOH treatment. However, the small domains with different elasticity may correspond not only to the presence of the 18-MEA layer but also to regions where solvent or humidity adsorbed efficiently.

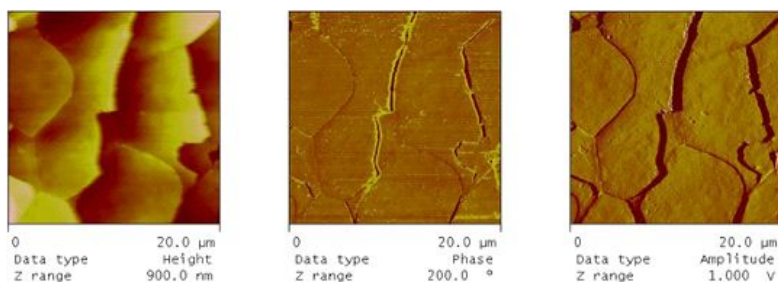
20x20 μm^2
scans



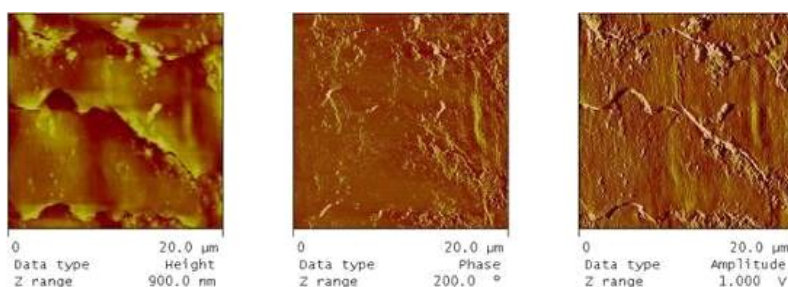
Light hair washed with water #1-1



Light hair treated with Acetonitrile #1-2



Light hair treated with KOH #1-3



Light hair treated with KMnO4 #1-4

Fig. 9: Typical scans of hair samples treated in four solvents. The left column corresponds to height changes; the middle column, to amplitude changes; and the right column, to phase changes. The top row shows scans of hair treated in distilled water only; the second row was rinsed in acetonitrile; the third row was in methanol-KOH solution; and the bottom row was rinsed in permanganate solution.

2x2 μm^2
scans

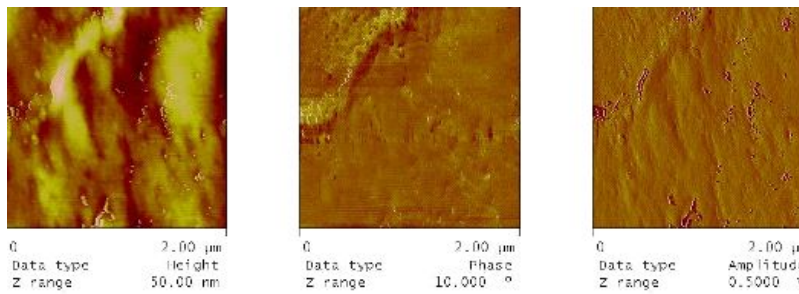
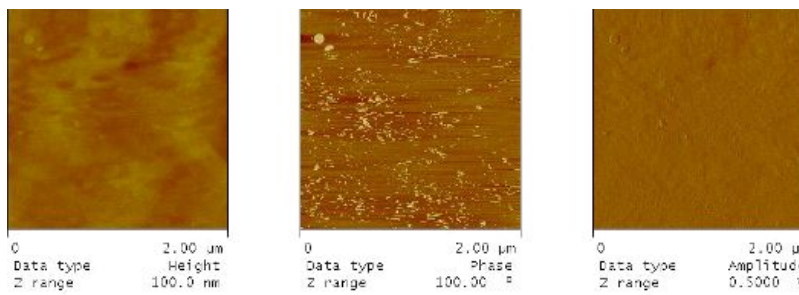
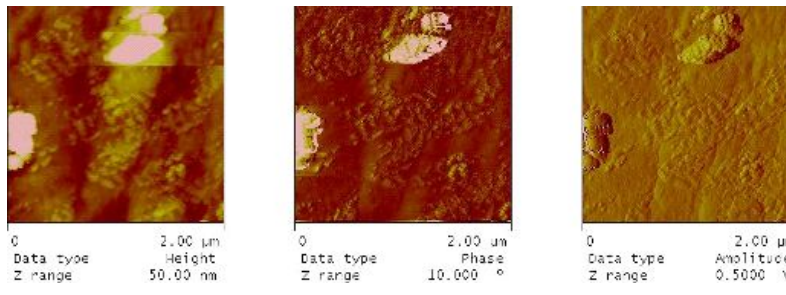
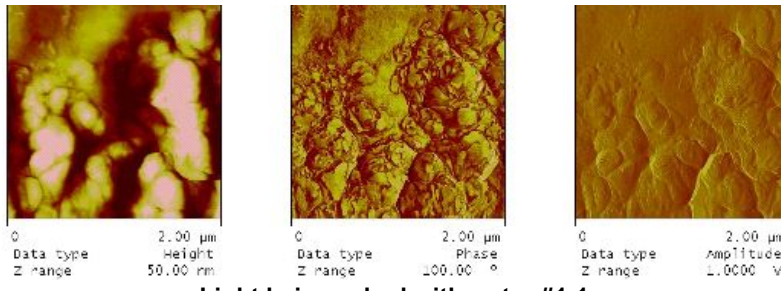


Fig. 10: Same format as Fig. 8 but the scan dimensions are ten times smaller.

Analysis of the height variation in these images (first column) is shown in Figure 11. The analysis of height variation in the scanned region includes the mean value of the heights in the image, the root mean square height being defined by:

$$R_q = \sqrt{\frac{\sum_i Z_i^2}{N}}$$

and the arithmetic average of the absolute values of the surface height deviations measured from the mean plane, R_a , defined by:

$$R_a = \frac{1}{N} \sum_{i=1}^N |Z_i|$$

and where N is the number of points whose height, Z_i , are measured in the scan.

Figure 11 shows the degree of roughness in these $(2\mu\text{m})^2$ scanned areas. The principle measure is the value of R_a . In the case of samples rinsed in distilled water only, R_a equals 13.1 nm, while for methanol-KOH treatment the observed value reduces to 1.8 nm. The corresponding values for the other two samples are in between these two values. The R_a value obtained for the methanol-KOH treated samples seem to be even smaller than the width of the 18-MEA layer, another indication to its absence after the solvent treatment.

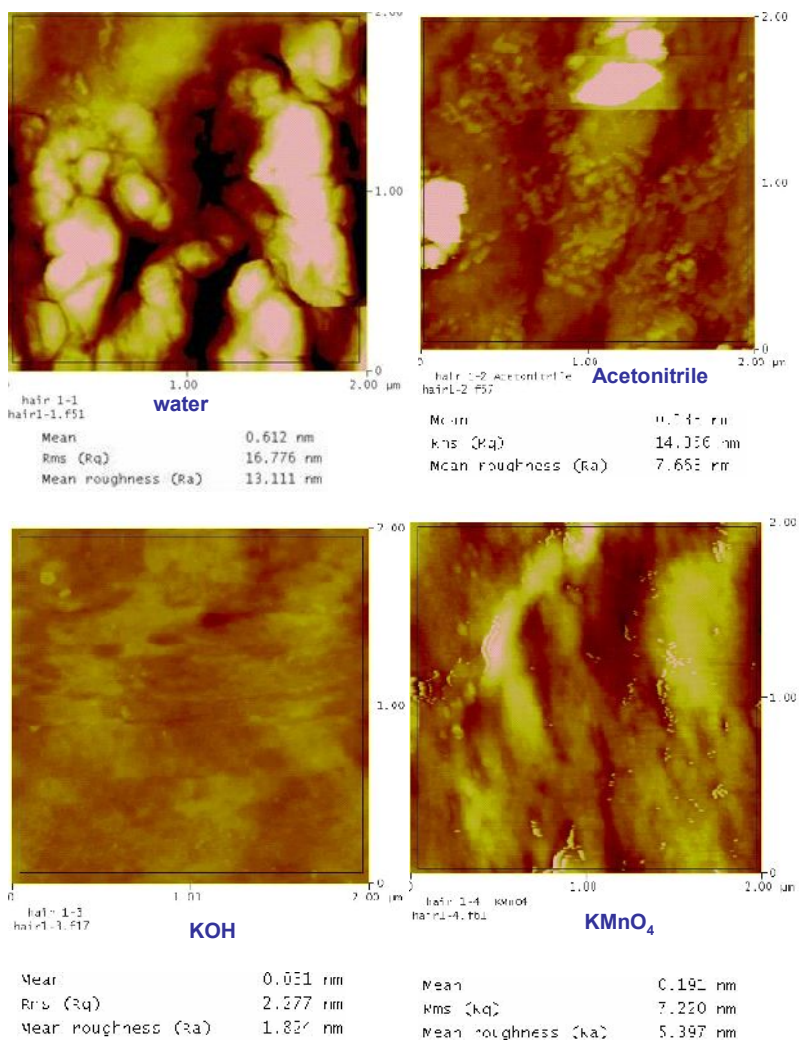


Fig. 11: Roughness measures of the four samples.

The TM-AFM photographs clearly show that all bleaching treatments examined reduce the hair surface roughness. This reduced roughness leads to a decreased sorption of both TATP and TNT on the hair surface. Yet, the sorption of these two explosives differs. Apparently, TATP nucleates more readily than TNT. DFT calculations, described below, were used to determine possible mechanisms that may lead to TATP nucleation.

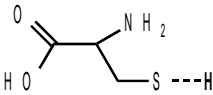
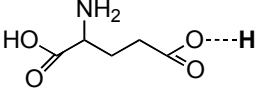
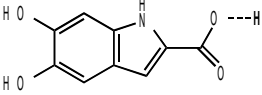
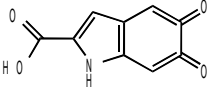
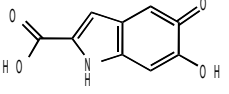
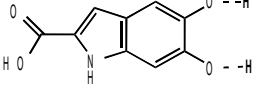
Possible nucleation of TATP micro-crystals

Our previous study showed that TATP physisorption on acidic centers is thermodynamically stable.⁹ The hydrogen bonds formed in most complexes were quite long and led to very small changes in the geometry and electronic structure of the TATP molecule. These results suggested that such

adsorption sites for TATP do not provide complexes that are stable enough to serve as nucleation sites. Furthermore, one would expect that nucleation sites will lead to much larger modification of the TATP structure and the charge distribution to provide efficient adsorption of molecular TATP onto the modified adsorbed molecule. Hence, one must examine configurations in which the initial adsorption leads to stable adsorbate that can induce further nucleation.

In the following we compare the TATP adsorption efficiency of different quinonic functional groups of melanin with those of glutamine and cystine units that are found on the hair protein surface (rows 1 and 2 in Table 4). This data clearly shows that both phenolic and acidic OH groups of hydroquinone (HQ) form very strong hydrogen bonds with TATP. Such strong hydrogen bonding may lead to hydrogen transfer from the HQ to the adsorbed TATP.

Table 4. DFT optimized hydrogen bond lengths ($d_{\text{O-H}}$, Å) & thermodynamic parameters (ΔH , kcal/mol & ΔG , kcal/mol at 298.15 K) for TATP interactions with functional groups of protein & melanin.

Group		Molecular structure	Physisorption properties		
			$d_{\text{O-H}}$	ΔH	ΔG^{298}
-SH	Cys		2.370	-3.64	+7.19
-COOH	Glu		2.327	-9.05	+5.16
-COOH	Hydroquinone (HQ)		1.805	-19.10	-6.98
-COOH	Ortho-quinone (OQ)			-2.45	
-OH	Semiquinone (SQ)		1.900	-4.99	
2(-OH)*	Hydroquinone (HQ)		1.950; 2.145	-17.56	-4.54

* - Two hydroquinone OH groups form two hydrogen bonds with TATP molecule.

Protonation of TATP is an exothermic process ($\text{TATP} + \text{H}^+ \rightarrow \text{TATP-H}^+$ $\Delta\text{H} = -216.0$ kcal/mol) leading to rupture of a C-O bond to form a terminal O-H and a carbon radical (Fig. 12). The resulting three-coordinated C-atom accepts large electron density (mainly from the nearest O-atom) and forms nearly a double bond with it. The resulting complex exhibits bond elongation and reduction in interatomic population of the C-OO bonds and strengthening of the O-O bonds. The HOMO of the complex is mainly localized on the O-atoms marked with stars in Fig. 12 and has π^* - nature with respect to this bond. However, proton abstraction by TATP from H_3O^+ is much less exothermic ($\text{TATP} + \text{H}_3\text{O}^+ \rightarrow \text{TATP-H}^+ + \text{H}_2\text{O}$: $\Delta\text{H} = -39.4$ kcal/mol). Proton abstraction from such weak acids as Cys and Glu is thermodynamically unfavorable ($\Delta\text{H} = +151.7$ and $+143.7$ kcal/mol; $\Delta\text{G} = +92.6$ and $+85.9$ kcal/mol, respectively). Such high endothermicity allows exclusion of TATP protonation by these sites on the hair surface. Chemisorption of the TATP molecule by addition of a S-H bond of Cys (Fig. 13) across the C-O bond was also found to be energetically highly unfavorable.

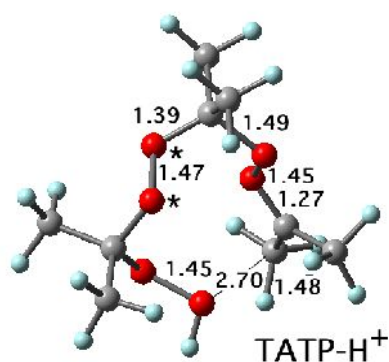
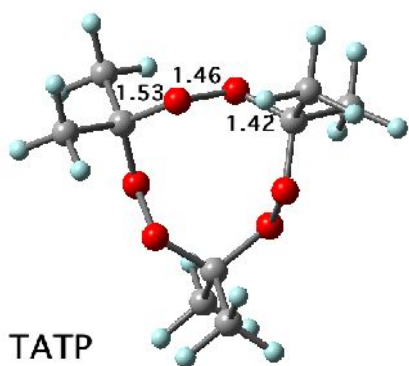


Fig. 12: TATP and TATP-H⁺ geometries optimized at the B3LYP/cc-pVDZ level of theory. Also shown are some important bond lengths.

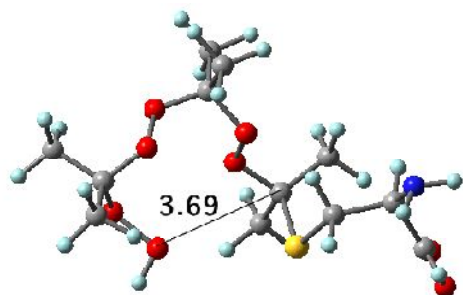
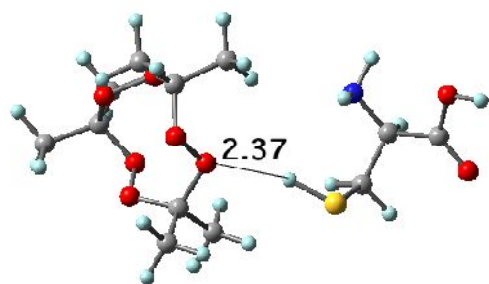


Fig. 13: TATP interactions with cysteine (Cys): H-bond formation (top) & S-H addition across C-O bond (bottom).

Another type of possible TATP activation is by interaction with radical centers presented on hair surface (cysteine) and in melanin granules. Radical interactions of TATP could proceed several ways. Excitation of the molecule to the triplet state is thermodynamically unfavorable ($\Delta H = +33.02$ kcal/mol, $\Delta G^{298} = +25.95$ kcal/mol). Homolytic decomposition is highly endothermic ($\Delta H = +108.1$ kcal/mol), but abstraction of H-atom by another radical can be energetically easier ($\Delta H = +0.8$ kcal/mol for hydrogen abstraction by a H atom). The preferential interaction of TATP with an H radical is attractive. It is characterized by a strong decrease in the product enthalpy (TATP + H (Fig. 14.I): $\Delta H = -77.18$ kcal/mol, $\Delta G^{298} = -68.15$ kcal/mol; TATP + 2H (Fig. 14.II): $\Delta H = -79.9$ kcal/mol, $\Delta G^{298} = -66.32$ kcal/mol). These interactions with a single or two H atoms leads to rupture of one O-O bond and elongation of the other O-O and several C-O bonds (Fig. 14). In the following we shall term the products in these two reactions as product I and product II. The first interaction present the formation of a radical nucleation center while the second one presents rupture of a radical chain. Exothermicities of these reactions are not enough to brake the S-H bond in the cystine aminoacid [reaction (1) in Table 5]. Even the formation of a disulfide bond could not compensate the endothermicity associated with two H atom transfer reaction [reaction (2) in Table 5]. On the other hand, hydrogen abstraction reaction upon TATP adsorptions onto semiquinone (SQ) or hydroquinone (HQ) sites are energetically favorable (reactions 3-7 in Table 5).

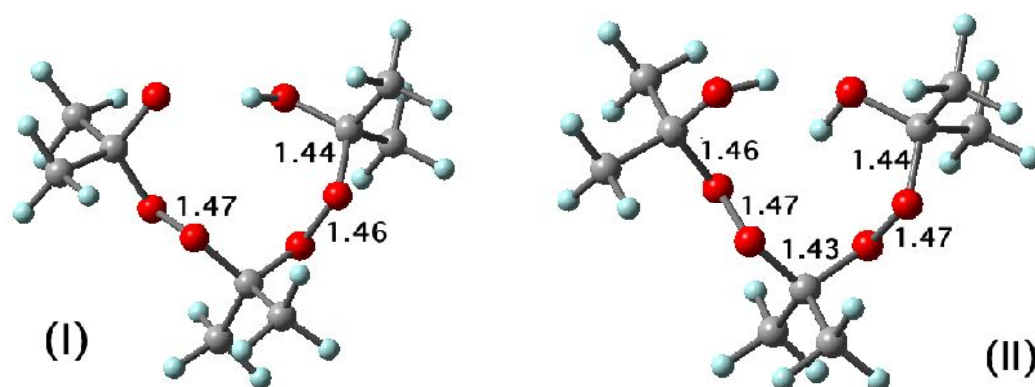


Fig. 14: TATP-H (I) and TATP-2H (II) geometries optimized at the B3LYP/cc-pVDZ level of theory. Also shown are some important bond lengths

Table 5. Thermodynamics of H atom abstraction by TATP molecules

		ΔH , kcal/mol	ΔG^{298} , kcal/mol
1	$\text{P-SH} + \text{TATP} \rightarrow \text{P-S} + (\text{I})$	12.19	7.96
2	$2\text{Cys} + \text{TATP} \rightarrow \text{Cys}_2 + (\text{II})$	16.87	21.24
3	$\text{SQ} + \text{TATP} \rightarrow \text{OQ} + (\text{I})$	4.99	-0.19
4	$\text{HQ} + \text{TATP} \rightarrow \text{SQ} + (\text{I})$	-0.98	-6.38
5	$\text{HQ} + \text{TATP} \rightarrow \text{OQ} + (\text{II})$	-28.89	-31.56
6	$\text{SQ} + (\text{I}) \rightarrow \text{OQ} + (\text{II})$	-27.91	-25.18
7	$\text{HQ} + (\text{I}) \rightarrow \text{SQ} + (\text{II})$	-33.88	-31.37

The radical product I in reactions 3 and 4 (Table 5) exhibit higher affinity to form dimers with another TATP molecule (Fig. 15) than a closed shell TATP (ΔH for formation of $(\text{TATP})_2$ and TATP-(I) dimers are -2.26 and -4.17 kcal/mol, respectively.). These results suggest that product I species may serve as possible nucleation sites for TATP if the gas phase is saturated with TATP. At room temperature, both TATP-TATP and TATP-(I) complexes become thermodynamically unfavorable due to the entropy effects. This is in agreement with the observed high vapor pressure of TATP at room temperature. Calculated ΔG^{298} values (+8.42 and +8.08 kcal/mol for $(\text{TATP})_2$ and TATP-product I dimers, respectively) suggest that, in equilibrium with the saturated gas phase, TATP molecules will adsorb onto radical sites 1.77 times faster as compared to adsorption onto TATP crystallites. The dimer TATP-(I) remains a radical in nature; therefore, it continues to attract additional TATP molecules.

The most stable complex is formed between two product I radicals ($\Delta H = -29.40$ kcal/mol, $\Delta G^{298} = -10.64$ kcal/mol). This complex can also serve as a nucleation site for TATP; however, it does not possess a radical nature; hence, its ability to further adsorb additional TATP molecules should be similar to that of TATP crystallites.

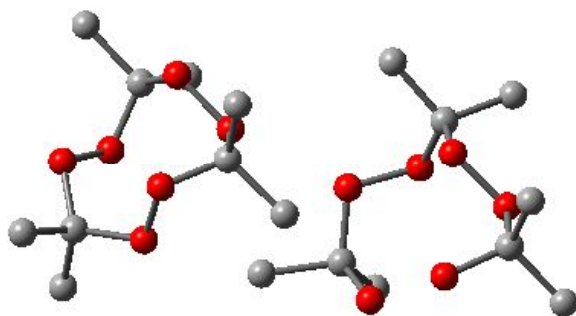


Fig. 15: Optimized (TATP-H-TATP) (complex (TATP-I)) dimer geometry. Hydrogen atoms are omitted for clarity.

The computational results discussed above allow exclusion of acidic and cystine/cysteine centers as possible TATP nucleation centers. From chemical viewpoint, melanin centers are able to initiate nucleation of TATP micro-crystallites. However, the fact that melanin granules are located inside the hair shaft makes such interaction unfeasible. Recently it was found that, despite the similar biochemical composition of human hair among different races¹⁹, physico-morphological characteristics are not identical in different ethnic groups.²⁵ In particular, (i) large melanin granules were found in black hair in the cortex layer;²⁶ (ii) the amounts of fibrous proteins and matrix substances differ in the hair of different races (the FP/MS ratios obtained from the Mongoloid hair were 0.45 ± 0.03 ; those from the Negroid, 0.18 ± 0.02 ; and those from the Caucasoid, 0.29 ± 0.02). These differences do not affect the distribution of the cystine-rich proteins.²⁷ One would expect that penetration of molecules through the hair surface is more difficult for Asian origin hair as it has more cuticle layers and wider cuticle cells than Caucasian hair. In addition, the cuticular inclination of Asian hair is steeper and its cuticular interval is narrower than in Caucasian hair.²⁸ However, recent study demonstrated that the cuticles of Asian hair are more easily peeled off than Caucasian hair cuticles during daily grooming.²⁹ This

finding together with high abundance of melanin granules in the near-surface hair layers allow to suggest that interaction between melanin and TATP molecules takes place at defects or damage sites on black hair. This hypothesis is supported by wide individual variation in the adsorption properties of black hair (see Table 1). Physisorption of explosive molecules within the lipid layer on hair surface could also provide nucleation centers at which explosive molecules can condensate in equilibrium with saturated gas phase to form nucleation centers for micro-crystals. However, these centers are less active than radical centers. Significant acidity of adsorption sites on melanin granule surface may play an important role in the coordination of explosive molecules at such sites prior to their nucleation. On the other hand, adsorption of polar solvent molecules, such as acetonitrile and methanol, showing both hydrophilic and hydrophobic affinity, could result in blocking of most melanin nucleation centers present on hair surface. This is expected to markedly reduce radical-induced nucleation of TATP micro-crystallites. However, it is expected to have only a minor effect on TNT adsorption which is driven preferentially by van der Waals and ionic interactions.

.Conclusions

In this study hair was treated in a number of ways: moistening; rinsing with acetonitrile or methanol; bleaching with hydrogen peroxide and alkaline hydrogen peroxide; treating with a methanolic KOH solution or potassium permanganate. Bleaching the hair greatly reduced sorption of TATP and TNT to hair. However, treatments which had no effect on hair color had differing effects on TATP and TNT. For example, rinsing with acetonitrile or methanol drastically lowered the sorption of TATP, while having little effect on TNT. These observations, along with those previously reported in differential extraction experiments; may suggest that TATP attachment to hair is mainly a surface phenomenon, while TNT may have also an inner core sorption. The theoretical calculations discussed above may suggest that the experimental findings could also be related to the efficient adsorption of solvent molecules to melanin sites. TM-AFM micrographs reveal surface structural changes due to the various treatments of hair. Together with the other results presented herein this supports the

hypothesis that 18-MEA lipid layer plays a major role in explosive sorption. DFT calculations were employed to explain the extremely high TATP adsorption by several samples of black hair. It has been demonstrated above that TATP interactions with radical centers on melanin surface could lead to formation of microcrystallites when the hair is exposed to TATP saturated gas phase. The marked reduction of TATP sorption by pre-treatment with acetonitrile or methanol is attributed by the calculations to blocking of the radical centers on the melanin granule surface. Reduced sorption of TATP and TNT to bleached and grey hair is attributed to both disappearance of radical centers and destruction of the lipid layer on hair surface.

Acknowledgment

The authors thank NATO Science for Peace and Oklahoma Memorial Institute for Prevention of Terrorism (MIPT) for funding this work. YZ and IE thank the "Center for Security Science and Technology Research Centers" at the Technion for partial support of this work.

Footnote

2,4,6-trinitrotoluene (TNT); pentaerythritol tetranitrate (PETN); hexahydro-1,3,5-trinitro-s-triazine (RDX); and triacetone triperoxide (TATP); two, EGDN (ethylene glycol) and NG (nitroglycerin).

References

- ¹ Oxley, J.C.; Smith, J. L.; Kirschenbaum, L.; Shinde, K.; Marimnganti, S. “Accumulation of Explosives in Hair;” *J. Forensic Science*; **2005**, Vol 50, No. 4.
- ² Oxley, J.C.; Smith, J. L.; Kirschenbaum, L.; Marimnganti, S. “Accumulation of Explosive in Hair: Part 2;” *J. Forensic Science*; **2007**, Vol 52, No. 6.
- ³ Jones L N. “Hair structure anatomy and comparative anatomy.” *Clin. Dermatol.* **2001**, 19, 95-103.
- ⁴ Swift, J.A.; Smith, J.R. “Microscopic investigations on the epicuticle of mammalian keratin fibres.” *J. Microscopy.*, **2001**, 204, 203–211.
- ⁵ Evans, D.J., Leeder, J.D., Rippon, J.A. & Rivett, D.E. “Separation and analysis of the surface lipids of the wool fibre.” Proc. 7th Int. Wool Text.” *1985 Res. Conf. Tokyo*, 1, 135–142.
- ⁶ Smith, J. R. & Swift, J. A. “Lamellar subcomponents of the cuticular cell membrane complex of mammalian keratin fibres show friction and hardness contrast by AFM.” *J. Microscopy* **2002**, 206 (3), 182-193.
- ⁷ Negri, A. P.; Cornell, H. J.; Rivett, D. E. “Model for the surface of keratin fibers.” *Textile Research J.* **1993**, 63, 109-115.
- ⁸ Negri A.; Rankin D.A.; Nelson W.G.; Rivett D.E. “A transmission electron microscope study of covalently bound fatty acids in the cell membranes of wool fibers.” *Textile Research J.* **1996**, 66, 491-495.
- ⁹ Efremenko, I.; Zach, R.; Zeiri, Y. J. Phys. Chem. B, *J. Phys. Chem. C* **2007**, 111, 11903-11911.
- ¹⁰ Paul Meredith, Ben J. Powell, Jennifer Riesz, Stephen P. Nighswander-Rempel, Mark R. Pederson and Evan G. Moore, *Soft Matter*, 2006, 2, 37-44
- ¹¹ J.A. Swift and J.R. Smith, *Scanning* **2000**, 22, 310.
- ¹² a. C. LaTorre and B. Bhushan, *Ultramicroscopy* **2005**, 105, 115; b. C. LaTorre and B. Bhushan, *J. Vac. Sci. Technol.* **2005**, A23, 1034.
- ¹³ N. Chen and B. Bhushan, *Journal of Microscopy*, **2005**, 220, 96.
- ¹⁴ R.A. Lodge and B. Bhushan, *J. Vac. Sci. Technol.* **2006**, A24, 1258.

¹⁵ Frisch, M. J.; Trucks, G. W.; Schlegel, H. B.; Scuseria, G. E.; Robb, M. A.; Cheeseman, J. R.; Montgomery, Jr., J. A.; Vreven, T.; Kudin, K. N.; Burant, J. C.; Millam, J. M.; Iyengar, S. S.; Tomasi, J.; Barone, V.; Mennucci, B.; Cossi, M.; Scalmani, G.; Rega, N.; Petersson, G. A.; Nakatsuji, H.; Hada, M.; Ehara, M.; Toyota, K.; Fukuda, R.; Hasegawa, J.; Ishida, M.; Nakajima, T.; Honda, Y.; Kitao, O.; Nakai, H.; Klene, M.; Li, X.; Knox, J. E.; Hratchian, H. P.; Cross, J. B.; Bakken, V.; Adamo, C.; Jaramillo, J.; Gomperts, R.; Stratmann, R. E.; Yazyev, O.; Austin, A. J.; Cammi, R.; Pomelli, C.; Ochterski, J. W.; Ayala, P. Y.; Morokuma, K.; Voth, G. A.; Salvador, P.; Dannenberg, J. J.; Zakrzewski, V. G.; Dapprich, S.; Daniels, A. D.; Strain, M. C.; Farkas, O.; Malick, D. K.; Rabuck, A. D.; Raghavachari, K.; Foresman, J. B.; Ortiz, J. V.; Cui, Q.; Baboul, A. G.; Clifford, S.; Cioslowski, J.; Stefanov, B. B.; Liu, G.; Liashenko, A.; Piskorz, P.; Komaromi, I.; Martin, R. L.; Fox, D. J.; Keith, T.; Al-Laham, M. A.; Peng, C. Y.; Nanayakkara, A.; Challacombe, M.; Gill, P. M. W.; Johnson, B.; Chen, W.; Wong, M. W.; Gonzalez, C.; and Pople, J. A. Gaussian 03, Revision C.01wis5, (WIS customized version 5) Gaussian, Inc., Wallingford CT, 2004.

¹⁶ Prota G. *Pigment Cell Res.* 13,2000, 283.

¹⁷ P. A. Riley. *The International Journal of Biochemistry & Cell Biology*, 29, 1997, 1235-1239.

¹⁸ Kalyanaraman B., Felix C.C., Sealy R.C. (1984). *J. Amer. Chem. Soc.* 106, N 24, 7327-7330.

¹⁹ See for example: a) B. J. Kim, J. I. Na, W. S. Park, H. C. Eun, O. S. Kwon *Int. J. Dermatology* 45, 1435, 2006. b) Paul Meredith, Ben J. Powell, Jennifer Riesz, Stephen P. Nighswander-Rempel, Mark R. Pederson and Evan G. Moore. *Soft Matter*, 2, 2006, 37.

²⁰ Robbins, C.R. "Chemical and Physical Behavior of Human Hair" 3rd ed Springer-Verlag **1994**, pp 64-65, 133-146.

²¹ See for example: a) Wolfram L.J. *J. Soc Cosmetic Chem.* **1970**, 21, 875; b) Wolfram L.J.; Hall K. *J. Soc Cosmetic Chem.* **1975**, 26, 247.

²² Robbins, C.R.; Kelly, C.H. *J. Soc Cosmetic Chem.* **1969**, 20:555.

²³ Zahn, H. *J. Soc. Cosmetic Chem.* **1966**, 17, 687.

- ²⁴ Breakspear, S. Smith, J.R.; Luengo, G. “Effect of Covalently Linked Fatty Acid 18-MEA on the Nanotribology of the Hair’s Outer Surface” *J of Structural Biology* **2005**, 149, 235-242.
- ²⁵ See for example: (a) Franbourg A, Hallegot P, Baltenneck F, et al. Current research on ethnic hair. *J Am Acad Dermatol* 2003; 48: S115–S119. (b) Menkart J, Wolfram LJ, Mao I. Caucasian hair, Negro hair and wool: similarities and differences. *J Soc Cosmet Chem* 1984; 35: 21–43. (c) Lindelof B, Forslind B, Hedblad MA, Kaveus U. *Arch Dermatol.* 1988 Sep;124(9):1359-63.
- ²⁶ See for example: (a) Susan C. Taylor, *Skin of color: Biology, structure, function, and implications for dermatologic disease.* (b) D. P. Chakraborty and Shyamali Roy. *CHEMICAL AND BIOLOGICAL ASPECTS OF MELANIN • The Alkaloids, Volume 60, 2003, Pages 345-391.*
- ²⁷ N. P. Khumalo, R. P. R. Dawber, D. J. P. Ferguson (2005) *Experimental Dermatology* 14 (4), 311–314.
- ²⁸ Aubry A. F. “Applications of affinity chromatography to the study of drug-melanin binding interactions” *J. Chromatogr B Analyt Technol Biomed Life Sci.* **2002**;768(1):67-74.
- ²⁹ See for Example: (a) Joseph R.E., Tsai W.J., Tsao L.I., Su T.P., Cone E.J. *J. Pharmacology & Experimental Therapeutics* **1997**, 282, 1228-1241. (b) Slawson M.H.; Wilkins D.G.; Rollins D.E. *J Anal Toxicol.* **1998**, 6, 406-13. (c) Mars U.; Larsson, B.S. “Pheomelanin as a binding site for drugs and chemicals” *Pigment Cell Res.* **1999**;12(4):266-74.